AMERICAN SOCIETY FOR MICROBIOLOGY | Molecular and Cellular Biology

NFAT2 Isoforms Differentially Regulate Gene Expression, Cell Death, and Transformation through Alternative N-Terminal Domains

Pedro I. Lucena,[a] Douglas V. Faget,[a] Emilia Pachulec,[a] Marcela C. Robaina,[b] Claudete E. Klumb,[b] Bruno K. Robbs,[a]* João P. B. Viola[a]

Program of Cellular Biology, Brazilian National Cancer Institute (INCA), Rio de Janeiro, RJ, Brazil[a]; Program of Molecular Hemato-Oncology, Brazilian National Cancer Institute (INCA), Rio de Janeiro, RJ, Brazil[b]

The NFAT (nuclear factor of activated T cells) family of transcription factors is composed of four calcium-responsive proteins (NFAT1 to -4). The NFAT2 (also called NFATc1) gene encodes the isoforms NFAT2α and NFAT2β that result mainly from alternative initiation exons that provide two different N-terminal transactivation domains. However, the specific roles of the NFAT2 isoforms in cell physiology remain unclear. Because previous studies have shown oncogenic potential for NFAT2, this study emphasized the role of the NFAT2 isoforms in cell transformation. Here, we show that a constitutively active form of NFAT2α (CA-NFAT2α) and CA-NFAT2β distinctly control death and transformation in NIH 3T3 cells. While CA-NFAT2α strongly induces cell transformation, CA-NFAT2β leads to reduced cell proliferation and intense cell death through the upregulation of tumor necrosis factor alpha (TNF-α). CA-NFAT2β also increases cell death and upregulates Fas ligand (FasL) and TNF-α in CD4$^+$ T cells. Furthermore, we demonstrate that differential roles of NFAT2 isoforms in NIH 3T3 cells depend on the N-terminal domain, where the NFAT2β-specific N-terminal acidic motif is necessary to induce cell death. Interestingly, the NFAT2α isoform is upregulated in Burkitt lymphomas, suggesting an isoform-specific involvement of NFAT2 in cancer development. Finally, our data suggest that alternative N-terminal domains of NFAT2 could provide differential mechanisms for the control of cellular functions.

Nuclear factor of activated T cells (NFAT) was originally described as an essential transcription factor for T cell activation and differentiation (1). The NFAT family is composed of four calcium-responsive proteins, named NFAT1 (also called NFATc2/NFATp), NFAT2 (NFATc1/NFATc), NFAT3 (NFATc4), and NFAT4 (NFATc3/NFATx) (2–5), each displaying several splice variants (6, 7). These NFAT proteins have two conserved domains: the DNA-binding domain (DBD), which is the hallmark family domain, and the calcium-responsive N-terminal regulatory domain, denominated the NFAT homology region (NHR) (6).

Despite the conservation of the DBD and NHR, divergent phenotypes of NFAT-deficient mice suggest that different members of this family display nonredundant roles in cellular homeostasis (8). Apparently, NFAT1 and NFAT2 proteins have distinct roles in cell transformation, acting as a tumor suppressor and an oncogene, respectively (9). The tissue-restricted expression of the NFAT family members and isoforms supports the idea that these proteins might have cell-specific and/or gene-specific activities (7). The DBD and NHR conserved domains are flanked by the amino- and carboxy-terminal transactivation domains (TAD-N and TAD-C, respectively). These domains are highly variable regions between the NFAT family members and isoforms (6, 7). One hypothesis is that the differences between the TADs could be relevant for nonredundant functions of these transcription factors through the direct initiation of transcription or by cooperation with isoform-specific protein partners.

NFAT was described as an important regulator of genes involved in the control of the cell cycle and cell death, such as those for p21$^{WAF1/Cip1}$, cyclin-dependend kinase 4, c-myc, cyclin A2, Fas ligand (FasL), Nur77, c-FLIP, and tumor necrosis factor alpha (TNF-α) (10–17). Additionally, deregulation of calcineurin/NFAT signaling and abnormal expression of its components have been reported for several solid tumors, lymphomas, and leukemias (18, 19). Several studies have suggested the oncogenic potential of the NFAT family member NFAT2. NFAT2 was fundamental for pancreatic cancer progression and contributed to the survival of melanoma cells and the metastatic potential of colorectal cancer cells (11, 20, 21). Furthermore, NFAT2 was activated in 70% of Burkitt lymphoma cases and in ~30% of diffuse large B cell lymphoma (DLBCL) cases and was overexpressed and activated in cases of chronic lymphocytic leukemia (CLL) (22, 23).

The NFAT2 gene encodes the isoforms NFAT2α and NFAT2β that result mainly from the alternative 5′ initiation exons that provide two different TAD-Ns (24). While it has been demonstrated that different NFAT2 isoforms can be specifically regulated and expressed in T and B lymphocytes and mast cells, exhibiting differential roles in the regulation of cytokine expression (24–28), little is known about the specific roles of these isoforms in the regulation of cell death and tumor formation. Because NFAT2 displays important roles in tumorigenesis, we hypothesized that NFAT2 isoforms that diverge in the TAD-N may display differential functions in cellular transformation. To address this hypoth-

Received 13 May 2015 **Returned for modification** 5 July 2015
Accepted 8 October 2015

Accepted manuscript posted online 19 October 2015

Citation Lucena PI, Faget DV, Pachulec E, Robaina MC, Klumb CE, Robbs BK, Viola JPB. 2016. NFAT2 isoforms differentially regulate gene expression, cell death, and transformation through alternative N-terminal domains. Mol Cell Biol 36:119–131. doi:10.1128/MCB.00501-15.

Address correspondence to Bruno K. Robbs, brunokr@id.uff.br, or João P. B. Viola, jpviola@inca.gov.br.

* Present address: Bruno K. Robbs, Department of Basic Sciences, Fluminense Federal University (UFF), Nova Friburgo, RJ, Brazil.

esis, two constitutively active short NFAT2 isoforms (CA-NFAT2α and CA-NFAT2β) that diverge only in their N-terminal portions were overexpressed in nontransformed NIH 3T3 fibroblasts, and their role in cell transformation was analyzed. Surprisingly, while CA-NFAT2α acts as a positive regulator of cell proliferation in NIH 3T3 cells, inducing several hallmarks of transformation, CA-NFAT2β-expressing cells showed reduced cell proliferation and intense cell death through an increase in TNF-α cytokine expression levels. We demonstrated that an acidic activation domain (AAD) present in the TAD-N of CA-NFAT2β is essential for cell death induction by this isoform, such that substitutions of acidic amino acids within this domain completely abolish cell death and promote transformation. Furthermore, CA-NFAT2β was able to increase FasL and TNF-α levels and to induce cell death in $CD4^+$ T lymphocytes. Finally, a Burkitt lymphoma-derived cell line and human Burkitt lymphoma samples showed increased expression of the NFAT2α isoform, supporting the idea that this isoform contributes to cell transformation in cancer development. Taken together, these results suggest that NFAT2 isoforms have different roles in the control of cellular functions and that the transactivation domains may act as important regulators of nonredundant functions of the NFAT family members.

MATERIALS AND METHODS

Donors, patients, and Burkitt lymphoma samples. Human peripheral blood mononuclear cells (PBMCs) were obtained from 10 healthy blood donors at the blood bank of the Brazilian National Cancer Institute after written informed consent was obtained. The leukocytes were harvested from white blood cell reduction filters, and PBMCs were isolated by density gradient centrifugation using Ficoll. After written informed consent was obtained from each guardian, samples from seven cases of pediatric Burkitt lymphoma were included in this study. The samples were obtained from the Division of Pathology of the Brazilian National Cancer Institute. This study was approved by the Human Ethics Committee of the Brazilian National Cancer Institute (CEP process no. 018/09).

Cell culture. NIH 3T3, EcoPack2, Phoenix-ECO, and murine primary $CD4^+$ T cells were cultured in Dulbecco's modified Eagle's medium supplemented with $NaHCO_3$ (40 mM), NaH_2PO_4 (1 mM), sodium pyruvate (1 mM), minimum essential medium (MEM) vitamin solution (1×), MEM essential and nonessential amino acid solutions (1×), penicillin (100,000 U/liter), streptomycin (10 mg/liter), HEPES (10 mM), L-glutamine (2 mM), and β-mercaptoethanol (55 μM) (all from Gibco). Jurkat, 697, and Raji cells were cultured in RPMI medium supplemented with sodium pyruvate (1 mM), penicillin (100,000 U/liter), streptomycin (10 mg/liter), L-glutamine (2 mM), and β-mercaptoethanol (55 μM). All cultures were supplemented with 10% fetal bovine serum and incubated in a humidified environment containing 5% CO_2 at 37°C.

Animals. Athymic BALB/c nude, *Nfat2*$^{+/+}$ *Cd4-cre*$^{-}$, and *Nfat2*$^{fl/fl}$ *Cd4-cre*$^{+}$ mice were maintained at the Brazilian National Cancer Institute animal facility. *Nfat2*$^{fl/fl}$ *Cd4-cre*$^{+}$ mice were generated in Anjana Rao's laboratory (La Jolla Institute for Allergy and Immunology, San Diego, CA) (29). Eight- to twelve-week-old mice were used in all experiments, which were performed in accordance with the Brazilian Government's ethical and animal experiment regulations. The experiments were approved by and conducted according to animal welfare guidelines of the Ethics Committee of Animal Experimentation of the Brazilian National Cancer Institute (CEUA process no. 008/13 and 003/14).

$CD4^+$ T cell isolation. $CD4^+$ T cells were isolated from peripheral lymph nodes of *Nfat2*$^{+/+}$ *Cd4-cre*$^{-}$ or *Nfat2*$^{fl/fl}$ *Cd4-cre*$^{+}$ mice by negative selection using the Dynal Beads system (Invitrogen). $CD4^+$ cell purity was assessed by flow cytometry after isolation and was >95%.

Plasmid construction. The pLIRES-EGFP and pLIRES-EGFP-CA-NFAT2α vectors were constructed as previously described (9, 30). Murine CA-NFAT2β cDNA was a gift from Anjana Rao (31). Plasmid pLIRES-EGFP-CA-NFAT2β was constructed by subcloning CA-NFAT2β cDNA into the pLIRES-EGFP retroviral backbone plasmid using the restriction enzyme XhoI. The truncated CA-NFAT2-ΔN, CA-NFAT2β-Δ1-8, and CA-NFAT2β-Δ1-19 proteins were constructed by PCR amplification of the respective fragments of CA-NFAT2β cDNA followed by subcloning into the pLIRES-EGFP retroviral backbone. Plasmids pLIRES-EGFP-CA-NFAT2β-Δ9-19 and CA-NFAT2β-Mut-Acid were constructed by using the GeneTailor site-directed mutagenesis system (Invitrogen). CA-NFAT2β-Mut-Acid comprises the following amino acid substitutions: E9A, D11A, E17A, and D19A. The pRV-GFP vector was a gift from Anjana Rao. Plasmids pRV-GFP-CA-NFAT2α and pRV-GFP-CA-NFAT2β were constructed by subcloning CA-NFAT2α and CA-NFAT2β cDNAs, respectively, into the pRV-GFP retroviral backbone using the restriction enzymes SalI and XhoI. The bp −200 TNF-α promoter was synthesized (Genscript) and subcloned into the pGL4.10 vector (Promega). Plasmid κ3(long)-luciferase was acquired from Addgene (plasmid 11110) (32). The sequences of the primers used for plasmid construction are available upon request. All constructs were confirmed by DNA sequencing.

Production of recombinant retroviruses and infection of target cells. BD EcoPack2 ecotropic packaging cells (BD Biosciences) were transiently transfected with retroviral vectors by calcium phosphate precipitation for 24 h. The next day, the virus-containing supernatant was collected, mixed 1:1 (vol/vol) with fresh medium, supplemented with 8 μg/ml Polybrene (Fluka Chemie), and immediately used for spin infection of 2.5×10^4 NIH 3T3 cells in a six-well plate. After 24 h, the infected cells were trypsinized, and the efficiency of transduction was assessed by enhanced green fluorescent protein (EGFP) expression, which routinely revealed >85% virus-infected cells by flow cytometry. The time point of 24 h after transduction was defined as the starting point for all experiments using transduced NIH 3T3 cells. For transduction of primary $CD4^+$ T cells, Phoenix-ECO packaging cells were transiently transfected with retroviral vectors by calcium phosphate precipitation for 24 h. The next day, the virus-containing supernatant was collected and concentrated by centrifugation overnight at a relative centrifugal force (RCF) of 6,000 at 4°C. After concentration, the retroviruses were resuspended in fresh medium and supplemented with 8 μg/ml Polybrene. Primary $CD4^+$ T cells were stimulated with 1 μg/ml of anti-CD3 and 1 μg/ml of anti-CD28 (both from BD Pharmingen) in a 12-well plate coated with 0.3 mg/ml of goat anti-mouse IgG (MP Biomedicals). After 48 h, the culture medium was replaced with medium containing concentrated retrovirus, and $CD4^+$ T cells were spin infected. The conditioned lymphocyte medium was collected prior to the addition of virus, stored at 37°C, and added to the cells after spin infection. After 24 h, transduced cells were washed with phosphate-buffered saline (PBS), transferred to a six-well plate, and cultured with fresh medium supplemented with 20 U/ml of recombinant interleukin-2 (IL-2) (PeproTech) for 24 h. The time point of 48 h after transduction was defined as the starting point for experiments using transduced $CD4^+$ T cells. To ensure reproducibility, each experiment was repeated by using cells derived from independent virus infections.

Western blotting. Whole-protein extracts from transduced NIH 3T3 cells (1×10^5 cells) or $CD4^+$ T cells (1×10^6 cells) were obtained by cell lysis in buffer containing 40 mM Tris (pH 7.5), 60 mM sodium pyrophosphate, 10 mM EDTA, and 5% SDS, followed by incubation at 100°C for 15 min. Total cell lysates were resolved by SDS-PAGE, followed by transfer onto a nitrocellulose membrane. Immunodetection of NFAT2 variants, β-actin, and glyceraldehyde-3-phosphate dehydrogenase (GAPDH) was performed by using anti-NFATc1 monoclonal antibody 7A6 (Santa Cruz Biotechnology), anti-beta-actin polyclonal antibody (Abcam), and anti-GAPDH monoclonal antibody 6C5 (Santa Cruz Biotechnology), respectively, and visualized by using the SuperSignal West Pico chemiluminescent substrate (ThermoFisher Scientific).

Cell proliferation studies. NIH 3T3 cells were plated in triplicate into 96-well microtiter plates at a density of 8×10^3 cells/well. Cell proliferation was analyzed at the indicated times by crystal violet staining. The cells were fixed with ethanol, stained with 0.05% crystal violet in 20% ethanol, washed with distilled water, and solubilized with methanol. The optical density at 595 nm was read on a spectrophotometer.

Sub-G_0 analyses. NIH 3T3 cells were plated into a 12-well plate (1×10^5 cells/well). After 72 h, the cells were trypsinized and stained with propidium iodide (75 μM) in the presence of NP-40. Where indicated, CA-NFAT2β-expressing cells were treated with a TNF-α neutralizing antibody at a concentration of 1 to 1,000 ng/ml (catalog no. MCA1488XZ; AbD Serotec). DNA content was analyzed by collecting 10,000 events using a FACScalibur flow cytometer. Data were analyzed with CellQuest (BD Biosciences) and FlowJo (Tree Star Inc.) software.

Focus-forming assay and growth in semisolid medium. In the focus-forming assay, transduced NIH 3T3 cells were diluted 1:4 with uninfected wild-type NIH 3T3 cells and plated into a six-well plate at a final density of 5×10^4 cells/well. Growth medium was changed every 2 days. After 10 to 14 days, the cells were visualized by phase-contrast microscopy, and EGFP expression was detected by fluorescence microscopy. For visualization of foci, NIH 3T3 cells were fixed with ethanol and stained with 0.05% crystal violet in 20% ethanol. For growth in semisolid medium, transduced cells were resuspended in 0.4% agarose-supplemented growth medium and plated into six-well plates (5×10^3 cells/well) previously coated with 0.8% agarose-supplemented growth medium. After solidification, growth medium was added to each well, and the medium was changed every 3 days. After 4 to 5 weeks, the total number of colonies was determined by counting. Representative colonies were visualized by phase-contrast microscopy, and EGFP expression was detected by fluorescence microscopy.

Tumor formation. NIH 3T3 cells transduced with either control plasmid pLIRES-EGFP or pLIRES-EGFP-CA-NFAT2 were trypsinized and resuspended in PBS. Athymic 8- to 12-week-old BALB/c nude mice were injected subcutaneously in the right flank with 5×10^5 cells. Tumor volumes (V) were analyzed every 5 days by using the following formula: $V = 0.52 \times (\text{length}^2 \times \text{width})$. Mice were sacrificed, and photographs were taken 55 days after injection by using the Ivis Lumina XR Series III system (PerkinElmer) for the detection of EGFP expression in the tumors.

RNA extractions and real-time RT-PCR assays. Transduced NIH 3T3 cells were plated into 10-cm plates (1.5×10^6 cells/plate). After 16 h, total RNA was isolated by using RNeasy Mini Spin columns (Qiagen). First-strand DNA synthesis was performed by using the RT^2 first-strand kit (SABiosciences Corporation), and real-time PCR was performed by using SYBR green PCR master mix (SABiosciences). The PAMM-012 mouse apoptosis pathway RT^2 Profiler PCR array (SABiosciences) was used for expression analysis of 81 apoptosis-related genes, and the data were analyzed by using RT^2 Profiler PCR Array Data Analysis software (SABiosciences). For NFAT2 transcript analysis, primary $CD4^+$ T cells from C57BL/6 mice were cultured in six-well plates (3×10^6 cells/well) and stimulated with anti-CD3 and anti-CD28 (both at 1 μg/ml) for 1, 3, 24, and 48 h. Human cancer cell lines (Jurkat, 697, or Raji) were cultured in six-well plates (3×10^6 cells/well) and, when indicated, stimulated with phorbol myristate acetate (PMA) (10 nM) plus ionomycin (1 μM) for 4 h. For NFAT2 analysis using PBMCs from healthy donors, 1×10^7 freshly purified cells were used. Total RNA was isolated by using TRIzol LS reagent (Invitrogen), and first-strand cDNA was synthesized by using the ImProm-II reverse transcription (RT) system (Promega). Total RNA from paraffin-embedded tissue sections from seven cases of Burkitt lymphoma was isolated by using the RecoverAll total nucleic acid isolation kit for formalin- or paraformalin-fixed, paraffin-embedded tissues (Ambion), and first-strand cDNA was synthesized by using the High-Capacity cDNA reverse transcription (RT) kit (Applied Biosystems). Real-time PCR assays were performed by using SYBR green master mix (Applied Biosystems). The sequences of primers used for real-time PCR are available upon request. All procedures were performed according to the manufacturers' instructions.

ELISA. NIH 3T3 cells were plated into a 12-well plate at 1×10^5 cells/well, and $CD4^+$ T cells were cultured in a 24-well plate at 1×10^6 cells/well. The cell-free supernatant was collected after the indicated times, and TNF-α protein levels were assessed by using the murine TNF-α enzyme-linked immunosorbent assay (ELISA) development kit (PeproTech) according to the manufacturer's instructions.

Luciferase reporter assays. NIH 3T3 cells (5×10^4 cells/well in a six-well plate) were cotransfected with plasmid pGL4.10-TNF-α-promoter or κ3(long)-luciferase and a renilla plasmid (pRL-TK) by using the SuperFect transfection reagent (Qiagen). After 48 h, transfected cells were transduced with the indicated plasmid. On the following day, cells were plated into 12-well plates at a density of 1×10^5 cells/well. After 16 h, the cells were lysed with passive lysis buffer (Promega), and luciferase activity was analyzed by using a Dual-Luciferase reporter assay system (Promega) with a Veritas microplate luminometer (Turner Biosystems). The firefly luciferase reporter gene activity was normalized to renilla activity.

Annexin V staining. Transduced $CD4^+$ T cells were cultured in a 24-well plate at 1×10^6 cells/well and stimulated with PMA (10 nM) when indicated. After 6 h, the cells were collected, washed with PBS, resuspended in annexin V binding buffer (0.1 M HEPES [pH 7.4], 1.4 M NaCl, and 25 mM $CaCl_2$), and stained with annexin V-allophycocyanin (APC) (eBioscience) and 7-aminoactinomycin D (7-AAD) (BD Biosciences). Phosphatidylserine exposure was analyzed by collecting 10,000 EGFP-positive ($EGFP^+$) events by using a FACScalibur flow cytometer. Data were analyzed with CellQuest and FlowJo software.

FasL staining. Transduced $CD4^+$ T cells were cultured in a 24-well plate at 1×10^6 cells/well and stimulated with PMA (1 nM) when indicated. After 6 h, the cells were collected, washed with PBS, and stained with anti-FasL-phycoerythrin (PE) antibody (eBioscience). FasL levels were analyzed by collecting 10,000 $EGFP^+$ events using a BD Accuri C6 cytometer (BD Biosciences). Data were analyzed with BD Accuri C6 and FlowJo software.

Statistical analyses. Statistical analysis of values from control and treated groups was performed by using an unpaired Student t test for single comparisons or analysis of variance followed by the Student-Newman-Keuls test for multiple comparisons. The Mann-Whitney U test was used only when indicated for donor PBMC samples and patient Burkitt lymphoma samples. P values of ≤ 0.05 were considered statistically significant.

RESULTS

NFAT2 isoforms induce distinct phenotypes in NIH 3T3 cells. In order to characterize the roles of the NFAT transcription factors in cellular proliferation, we used previously described CA-NFAT2 mutants, which are known to be constitutively localized in the nucleus, to bind DNA with high affinity, and to activate endogenous NFAT target genes (9, 31). The use of constitutively active proteins allows the analysis of NFAT2 functions in the absence of external stimuli for NFAT activation that could activate other cellular pathways and mask NFAT-specific functions. Furthermore, the NIH 3T3 cell line was chosen because it is a classical model for studies of cell proliferation and transformation. Moreover, NIH 3T3 cells do not express NFAT2, providing a model for the analysis of specific NFAT2 variants. A schematic alignment of the NFAT2α and NFAT2β proteins is shown in Fig. 1A.

Initially, NIH 3T3 cells were infected with either an empty vector or a vector containing the cDNAs of the CA-NFAT2 isoforms (Fig. 1B), and the proliferation patterns were observed by a proliferation kinetic assay accompanied by a crystal violet incorporation assay. While control cells stopped growing once they reached confluence, CA-NFAT2α-expressing cells overgrew the monolayer and continued to proliferate beyond confluence (Fig. 1C). In contrast, CA-NFAT2β-expressing cells showed reduced

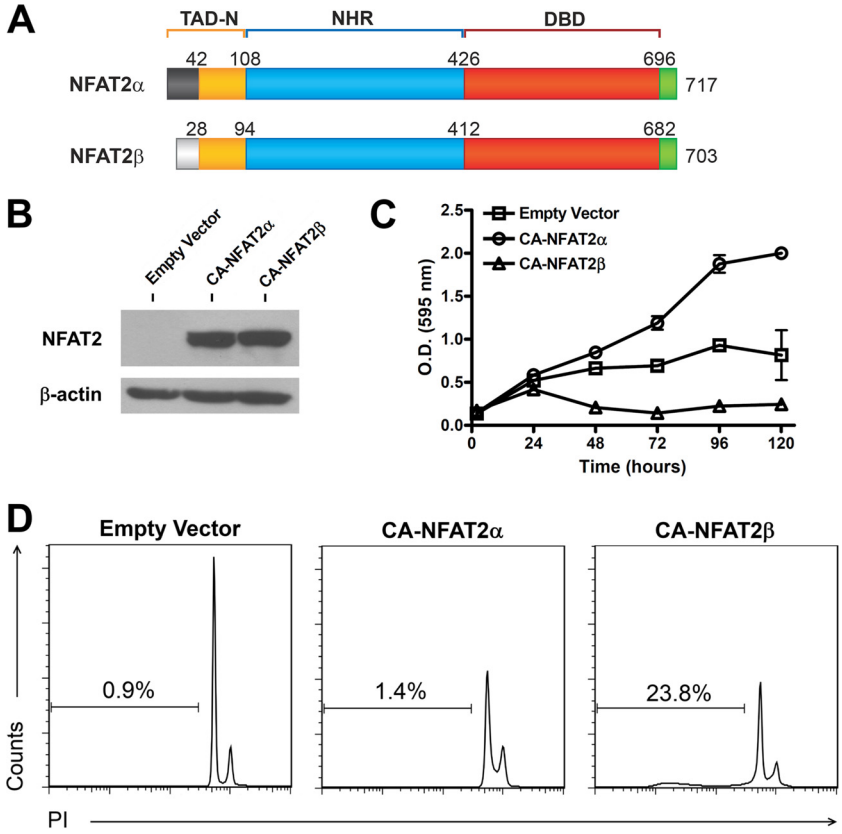

FIG 1 NFAT2 isoforms play different roles in cell proliferation and death in NIH 3T3 fibroblasts. NIH 3T3 cells were infected with either the control pLIRES-EGFP vector (empty vector) or the pLIRES-EGFP-CA-NFAT2 vector. (A) Schematic alignment of the NFAT2 short isoforms. The NFAT2α and NFAT2β proteins differ only at the N terminus, which contains 42 amino acids in the NFAT2α protein, encoded by exon 1 of the gene, or 28 differential amino acids in the NFAT2β protein, encoded by exon 2. The identical shading patterns represent identical sequences. The numbers indicate the amino acid positions in the murine proteins. DBD, DNA-binding domain; NHR, NFAT homology region; TAD-N, N-terminal transactivation domain. (B) Western blotting of transduced NIH 3T3 cells. (C) Proliferation kinetic assay by crystal violet staining. The data are presented as means ± standard deviations of results from one representative experiment. O.D., optical density. (D) Cell death analysis by propidium iodide (PI) staining 72 h after plating at confluence. The percentage of cell death (sub-G_0 DNA content) is indicated. All results are representative of data from at least three independent experiments.

cell accumulation and maintained a low-proliferation profile (Fig. 1C). To assess the cell death phenotype, sub-G_0 DNA content was analyzed. As shown by flow cytometry, ~20% of cells expressing CA-NFAT2β underwent apoptosis at 72 h postinfection, while cells expressing the control vector or CA-NFAT2α exhibited a low proportion of cell death (Fig. 1D). These results indicate that the NFAT2 short isoforms display distinct roles in controlling cell proliferation.

The observation that CA-NFAT2α leads to proliferation beyond confluence led to the question of whether the NFAT2 isoforms might exhibit distinct functions in cell transformation. The loss of contact-mediated growth inhibition was analyzed by a focus-forming assay in which transduced cells were mixed with an excess of uninfected wild-type NIH 3T3 cells. Whereas cells infected with the empty vector gave rise to a small number of foci, CA-NFAT2α-expressing cells formed a large number of foci (Fig. 2A). CA-NFAT2β-expressing cells also formed foci but induced less focus formation than did CA-NFAT2α-expressing cells (Fig. 2A). Analysis of EGFP expression showed that foci that formed in mixed cultures with either CA-NFAT2α- or CA-NFAT2β-expressing cells were composed of transduced cells (Fig. 2B). Furthermore, we tested whether the NFAT2 isoforms were able to induce the growth of NIH 3T3 cells in the absence of a solid substratum for adhesion. While control cells formed only small numbers of small colonies, CA-NFAT2α-expressing cells promptly formed many large colonies (Fig. 2C and D). Interestingly, although CA-NFAT2β expression in NIH 3T3 cells led to the formation of the same number of colonies as control cells, these colonies were larger (Fig. 2C and D). These results support the idea that while CA-NFAT2β expression can induce cell death in NIH 3T3 cells, those cells that survive its expression may acquire a transformed phenotype. Finally, cell transformation induced by NFAT2 isoforms was tested *in vivo*. Athymic mice receiving cells transduced with the empty vector did not give rise to any detectable tumor (Fig. 2E and F). However, CA-NFAT2α-infected cells promptly formed large tumors with a high growth rate in the flank of inoculated mice, while CA-NFAT2β-expressing cells formed only smaller and moderate-growing tumors (Fig. 2E and F). Additionally, tumors formed by CA-NFAT2β-expressing cells showed lower expression levels of EGFP than did CA-NFAT2α-expressing tumors (Fig. 2F), suggesting that they were composed of cells with lower CA-NFAT2β expression levels. Taken together, these results demonstrate that despite only a slight difference in the primary amino acid sequences between NFAT2α and NFAT2β, the

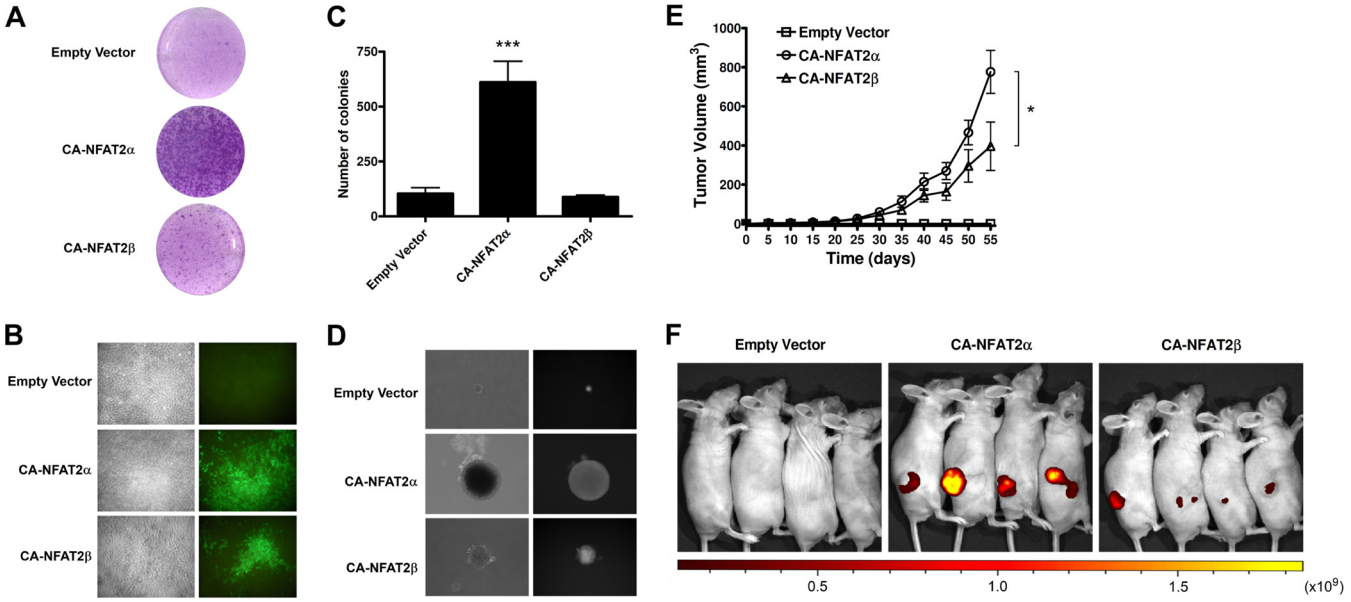

FIG 2 CA-NFAT2α and CA-NFAT2β induce cell transformation with distinct intensities in NIH 3T3 cells. Cells were transduced with the empty vector or vectors containing cDNAs of NFAT2 isoforms. (A) Focus-forming assay. Transduced cells were mixed 1:4 with uninfected wild-type NIH 3T3 cells and grown for 10 to 14 days. For visualization of foci, the cells were stained with crystal violet. (B) Phase-contrast microscopy (left) and optical fluorescence microscopy for EGFP expression (right) of representative foci. The results are representative of data from at least three independent experiments. (C) Growth in semisolid medium. Transduced NIH 3T3 cells were grown in semisolid agarose medium, and colonies were counted 4 to 5 weeks after plating. Data are shown as means ± standard deviations of results from three independent experiments. *** indicates a P value of ≤0.001. (D) Phase-contrast microscopy (left) and optical fluorescence microscopy for EGFP expression (right) of representative colonies. (E) Tumor formation in nude mice. NIH 3T3 cells (5×10^5 cells) were inoculated subcutaneously in the right flank of athymic BALB/c nude mice ($n = 7$). Tumor volumes were measured every 5 days, and the data are shown as means ± standard errors of the means. * indicates a P value of ≤0.05. (F) *In vivo* imaging of tumors from four representative mice 55 days after inoculation for EGFP expression. The color scale represents the fluorescence signal in radiance and ranges from red (minimum of 1.11×10^8 photons/s/cm^2/sr) to yellow (maximum of 1.85×10^9 photons/s/cm^2/sr).

expression of the alternative NFAT2 isoforms induces different phenotypes in NIH 3T3 cells. While NFAT2α positively controls cell proliferation and induces cell transformation, NFAT2β is able to induce cell death and a milder cell transformation phenotype.

The NFAT2 N-terminal differential domain enables cell death induction but is not necessary for transformation. As shown in Fig. 1A, NFAT2α and NFAT2β diverge only within the first amino acids of the TAD-N. In order to elucidate the role of the N termini of the NFAT2 isoforms in cell death and transformation, a truncated protein (CA-NFAT2-ΔN) that lacks only the amino acid residues that differ between the NFAT2α and NFAT2β isoforms was constructed (Fig. 3A) and expressed in NIH 3T3 cells (Fig. 3B). Strikingly, CA-NFAT2-ΔN-expressing NIH 3T3 cells showed a proliferation profile similar to that of CA-NFAT2α-expressing cells, leading to proliferation beyond confluence (Fig. 3C). Moreover, CA-NFAT2-ΔN-expressing cells showed a low proportion of cells undergoing apoptosis (Fig. 3D). Taken together, these results demonstrate that the differential 28-amino-acid (aa)-long N terminus of CA-NFAT2β is essential for the isoform-specific induction of cell death.

CA-NFAT2-ΔN-expressing cells induced a CA-NFAT2α-like cell transformation phenotype. CA-NFAT2-ΔN was able to promote the loss of contact-mediated growth inhibition, inducing the formation of numerous foci in the culture (Fig. 3E), and to promote anchorage-independent cell growth in semisolid medium (Fig. 3F and G). These data suggest that the differential TAD-N regions of the NFAT2 isoforms are not essential for cell transformation induced by NFAT2.

Conserved acidic amino acids in the N terminus of the NFAT2β protein are fundamental for induction of cell death. We have shown that the deletion of the first 28 aa of CA-NFAT2β completely abolished the induction of death in NIH 3T3 cells. The NFAT2β-specific amino terminus contains 7 acidic residues (Asp/Glu) interspersed with a number of hydrophobic residues, a pattern conserved in many acidic activation domains (AADs) (33). An alignment of the N termini of NFAT2β and the other NFAT family members revealed the conservation of several acidic/hydrophobic residues (Fig. 4A). In order to understand the importance of this domain for cell death, we constructed three truncated proteins that lacked amino acid residues 1 to 8, 1 to 19, and 9 to 19, termed CA-NFAT2β-Δ1-8, CA-NFAT2β-Δ1-19, and CA-NFAT2β-Δ9-19, respectively (Fig. 4B), and these constructs were expressed in NIH 3T3 cells (Fig. 4C). Surprisingly, only truncated proteins that lacked the acidic domain (CA-NFAT2β-Δ1-19 and CA-NFAT2β-Δ9-19) were unable to induce death in NIH 3T3 cells, while the deletion of the first 8 aa that do not encompass the conserved acidic domain did not abrogate cell death (Fig. 4D). These data demonstrate that the conserved acidic activation domain within the CA-NFAT2β N terminus is fundamental to CA-NFAT2β-induced cell death.

Previous studies of *Saccharomyces cerevisiae* showed that acidic amino acid residues interspersed with hydrophobic residues are important for the formation of an amphipathic alpha helix and for the activation of transcription (34). To elucidate the role of specific amino acid residues in the AAD of CA-NFAT2β, 4 acidic amino acid residues within this domain that are conserved be-

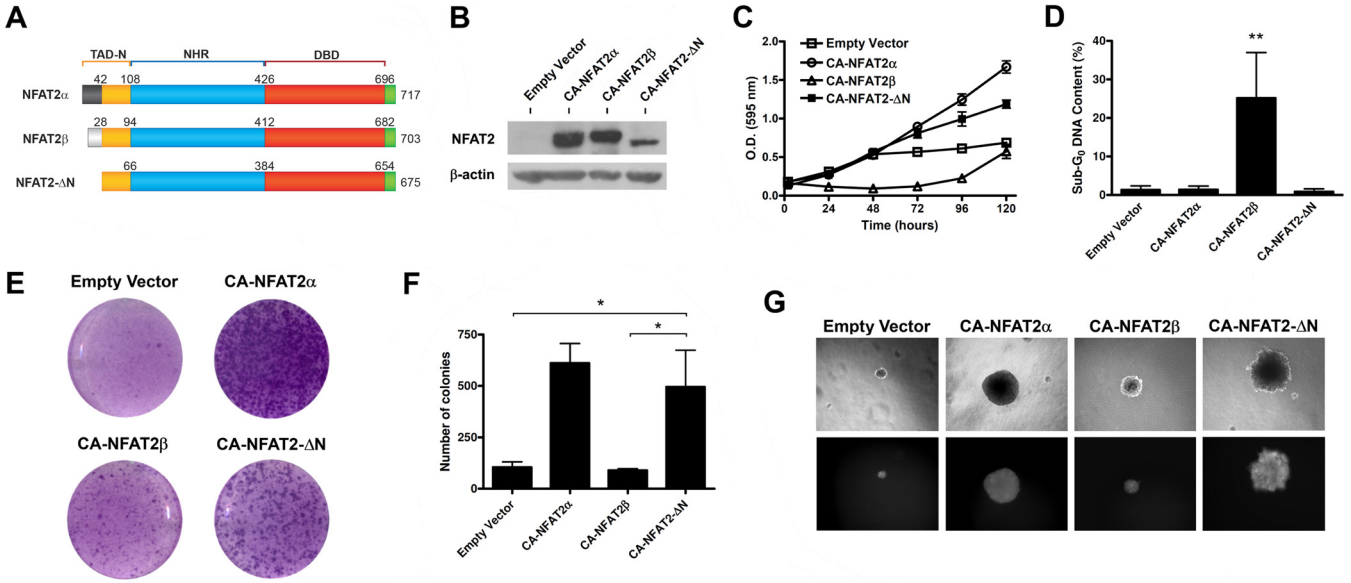

FIG 3 Cell death induction, but not cell transformation, is dependent on the NFAT2 N-terminal differential domain. NIH 3T3 cells were infected with either the empty vector or vectors containing cDNAs of the CA-NFAT2 variants. (A) Schematic alignment of the NFAT2 short isoforms and the truncated CA-NFAT2-ΔN protein. CA-NFAT2-ΔN lacks only the amino acid residues that differ between the NFAT2α and NFAT2β isoforms. (B) Western blotting of transduced NIH 3T3 cells. (C) Proliferation kinetic assay by crystal violet staining. O.D., optical density. The data are presented as means ± standard deviations of results from one representative experiment. (D) Cell death analysis by PI staining 72 h after plating at confluence. Standard deviation values indicate the variance of data from four independent experiments, and ** indicates a *P* value of ≤0.01. (E) Focus-forming assay. See the legend to Fig. 2A for details. (F and G) Growth in semisolid medium. Cells were cultured in semisolid agarose medium, and anchorage-independent cell growth was analyzed described in the legend to Fig. 2C and D. * indicates a *P* value of ≤0.05.

tween the NFAT proteins (Glu^{9}, Asp^{11}, Glu^{17}, and Asp^{19}) were mutated to noncharged alanine residues (CA-NFAT2β-Mut-Acid) (Fig. 5A). Comparison of the phenotypes induced by the CA-NFAT2 isoforms and CA-NFAT2β-Mut-Acid showed that mutations of only 4 amino acid residues of the AAD were sufficient to completely abolish CA-NFAT2β-induced cell death (Fig. 5B) and to increase cell accumulation (Fig. 5C). Cell transformation analyses demonstrated that CA-NFAT2β-Mut-Acid was able to induce increases in the numbers and sizes of the foci in culture and in colonies in semisolid medium (Fig. 5D to F). Taken together, these results suggest that the conserved acidic amino acids present in the NFAT2β-specific N-terminal domain are fundamental for the induction of cell death and that their ablation enhances the oncogenic potential of the NFAT2β protein.

CA-NFAT2β induces death of NIH 3T3 cells through upregulation of TNF-α. In order to determine which genes are regulated by CA-NFAT2β during cell death induction, we screened 81 apoptosis-related genes using a real-time PCR assay. Total RNA of NIH 3T3 cells was isolated 16 h after transduction with the different NFAT2 isoforms. This time point was chosen based on the lack of detectable cell death induced by CA-NFAT2β that could interfere with mRNA levels. Compared to control cells, CA-NFAT2α-expressing cells showed upregulation of 9 genes (*Bcl2l10*, *Naip1*, *Fasl*, *Il10*, *Pak7*, *Tnf*, *Cd40*, *Tnfsf10*, and *Cd70*) and downregulation of 1 gene (*Tnfrsf11b*), while CA-NFAT2β-expressing cells showed upregulation of 7 genes (*Fasl*, *Il10*, *Pak7*, *Tnf*, *Cd40*, *Cd70*, and *Trp73*) and downregulation of 5 genes (*Casp1*, *Casp12*, *Casp14*, *Tnfrsf11b*, and *Trp63*) (Fig. 6A). *Dapk1* and *Cd40lg* expression was undetectable in the samples. The overexpression of CA-NFAT2 isoforms affected mainly the expression of *Tnf*, *Fasl*, *Pak7*, and *Il10* (Fig. 6A). In addition, CA-NFAT2β expression led to greater increases in TNF-α (781-fold), FasL (120-fold), Pak7 (440-fold), and IL-10 (64-fold) mRNA levels than did CA-NFAT2α expression (147-, 9-, 66-, and 45-fold, respectively) (Fig. 6B). Because TNF-α and FasL are direct inducers of cell death through apoptosis, these proteins could account for cell death induction. Furthermore, previous work from our group showed that the accumulation of TNF-α can induce apoptosis in NIH 3T3 cells (17). Corroborating the increased mRNA levels, CA-NFAT2β led to a greater accumulation of TNF-α protein than did CA-NFAT2α and CA-NFAT2β-Mut-Acid (Fig. 6C), indicating that the N-terminal domain of NFAT2β is important for the upregulation of TNF-α. The TNF-α promoter contains several NFAT-binding sites (35), including a well-described κ3(long) element (Fig. 6D) (32). CA-NFAT2β was able to increase the transactivation of both the bp −200 TNF-α promoter and the κ3(long) element more than CA-NFAT2α and CA-NFAT2β-Mut-Acid (Fig. 6E). To analyze the importance of TNF-α expression for cell death induced by CA-NFAT2β, a neutralization assay was performed. TNF-α neutralization inhibited death in CA-NFAT2β-expressing cells in a dose-dependent manner to a maximum of ~70% inhibition (Fig. 6F). On other hand, CA-NFAT2α, CA-NFAT2β, and CA-NFAT2β-Mut-Acid induced slight increases in FasL protein levels, and FasL neutralization did not affect cell death induced by CA-NFAT2β (data not shown), indicating that FasL is not involved in CA-NFAT2β-induced death in NIH 3T3 cells. Taken together, these data suggest that CA-NFAT2β induces death in NIH 3T3 cells through the upregulation of TNF-α.

CA-NFAT2β induces cell death and upregulation of TNF-α and FasL in $CD4^{+}$ T cells. Previous studies demonstrated distinct expression patterns of NFAT2 isoforms (7, 24, 27). NFAT2β (short and long isoforms) is predominant in nonactivated lym-

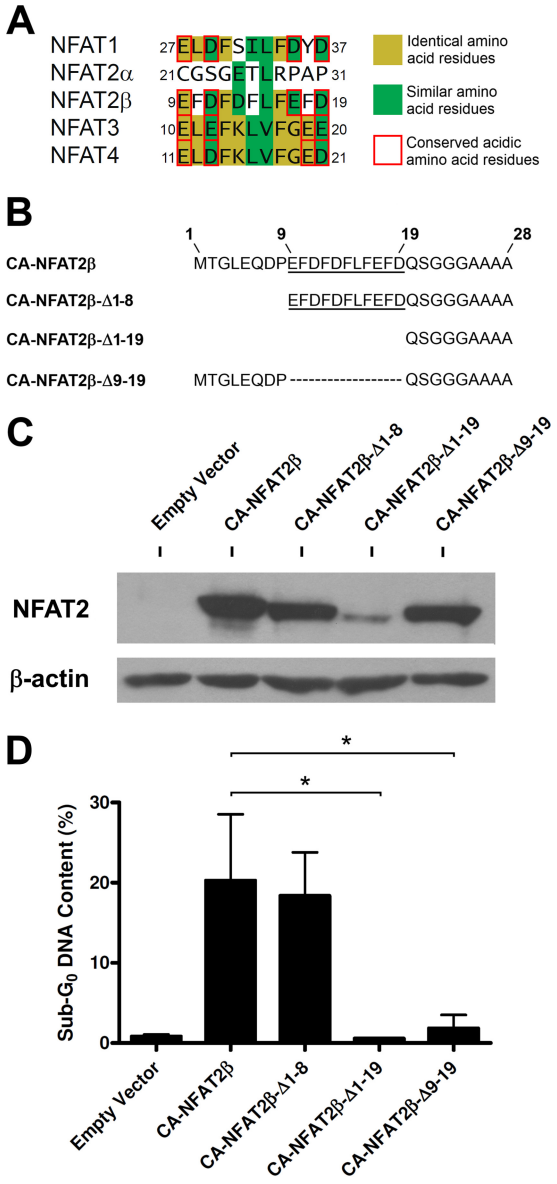

FIG 4 An acidic activation domain is fundamental for cell death induction by CA-NFAT2β. (A) Alignment of the N-terminal regions of the NFAT proteins. Amino acids encoded by the first exon of each NFAT gene were aligned by using the ClustalW tool. Shown is an acidic domain that displays sequence conservation between NFAT2β, NFAT1, NFAT3, and NFAT4 but not NFAT2α. The amino acid positions are indicated. (B) Schematic representation of the truncated variants of CA-NFAT2β. The conserved acidic domain is underlined. (C) Western blotting of transduced NIH 3T3 cells. (D) NIH 3T3 cells were transduced with either the empty vector or vectors containing full-length CA-NFAT2β or truncated CA-NFAT2β constructs. Cell death was analyzed by PI staining 72 h after plating at confluence. Standard deviation values indicate the variance of data from three independent experiments, and * indicates a P value of ≤ 0.05.

phocytes, while NFAT2α (mainly the short isoform) is upregulated after cell stimulation (Fig. 7A and B) (24, 25, 27). The increase in the NFAT2α level was associated with the entry of lymphocytes into the cell cycle without inducing cell death (24, 27). These data are compatible with our results with NIH 3T3 cells that suggest positive regulation of cell proliferation by NFAT2α, while NFAT2β negatively regulates cell proliferation and induces intense cell death.

In order to corroborate the differential roles of NFAT2 isoforms, we verified isoform-specific effects in $CD4^+$ T cells. *Nfat2*$^{fl/fl}$ *Cd4-cre*$^+$ mice are a T cell-specific *Nfat2* knockout model (29, 36) enabling the study of a role of the single NFAT2 isoform by reconstitution of $CD4^+$ T cells with the NFAT2-specific isoform. Primary $CD4^+$ T cells were purified from *Nfat2*$^{+/+}$ *Cd4-cre*$^-$ mice (wild-type cells) or *Nfat2*$^{fl/fl}$ *Cd4-cre*$^+$ mice (*Nfat2*$^{-/-}$ cells) and transduced with either plasmid pRV-GFP (empty vector), pRV-GFP-CA-NFAT2α, or pRV-GFP-CA-NFAT2β (Fig. 7C), and cell death profiles were analyzed by annexin V staining. While control cells (*Nfat2*$^{+/+}$ *Cd4-cre*$^-$ or *Nfat2*$^{fl/fl}$ *Cd4-cre*$^+$ $CD4^+$ T cells transduced with the empty vector) and CA-NFAT2α-expressing $CD4^+$ T cells (*Nfat2*$^{fl/fl}$ *Cd4-cre*$^+$ cells expressing CA-NFAT2α) showed a low proportion of apoptotic cells, CA-NFAT2β-expressing $CD4^+$ T cells (*Nfat2*$^{fl/fl}$ *Cd4-cre*$^+$ cells expressing CA-NFAT2β) showed increased cell death (~39% apoptotic cells) (Fig. 7D). The stimulation of NFAT transcriptional partner pathways (AP-1 and NF-κB) with PMA increased cell death induced by both NFAT2 isoforms (Fig. 7D) and led to the accumulation of the cytokine TNF-α (Fig. 7E). However, NFAT2 isoforms did not induce TNF-α production in the absence of PMA (Fig. 7E), suggesting that TNF-α is not sufficient to explain the differential roles of these isoforms in nonstimulated $CD4^+$ T cells. Furthermore, CA-NFAT2β-expressing cells showed increased FasL levels (Fig. 7F), which could account for the differences between the NFAT2 isoforms in cell death induction. These data suggest that NFAT2 isoforms have distinct roles in cell death in $CD4^+$ T lymphocytes, where CA-NFAT2β leads to a cell death phenotype that correlates with FasL and TNF-α upregulation.

NFAT2 isoforms are differentially expressed in Burkitt lymphomas. Some studies have indicated an involvement of NFAT2 in several hematological malignancies (18, 22, 23). As our data indicated distinct roles of the NFAT2 isoforms in the cellular transformation process in NIH 3T3 cells, we investigated the expression of the isoforms in cancer cell lines and tumors in order to reinforce an isoform-specific role in cancer development in alternative models. Three cancer cell lines were analyzed: Jurkat (T cell leukemia), 697 (pre-B cell leukemia), and Raji (Burkitt lymphoma). Similar levels of NFAT2α and NFAT2β mRNAs were observed in Jurkat and 697 cells, whereas Raji cells showed increased levels of the NFAT2α isoform compared to NFAT2β (Fig. 8A). All three cell lines showed an increase in NFAT2α expression after PMA and ionomycin stimulation (Fig. 8B). In addition, Burkitt lymphoma samples from patients showed high levels of NFAT2α, which were correlated with low levels of NFAT2β in the same sample, while peripheral blood mononuclear cells (PBMCs) from health donors showed lower levels of NFAT2α than of NFAT2β (Fig. 8C). Taken together, these data suggest a protumorigenic role of NFAT2α in Burkitt lymphomas.

DISCUSSION

Only a few studies have analyzed the phenotypic differences between the distinct NFAT isoforms. The NFAT2 isoforms display cell- and activation-specific expression patterns, suggesting different functions for these proteins. NFAT2 variants have alternative initiation exons that result in a change of the transcription start site from exon 2 to exon 1 to form the NFAT2β

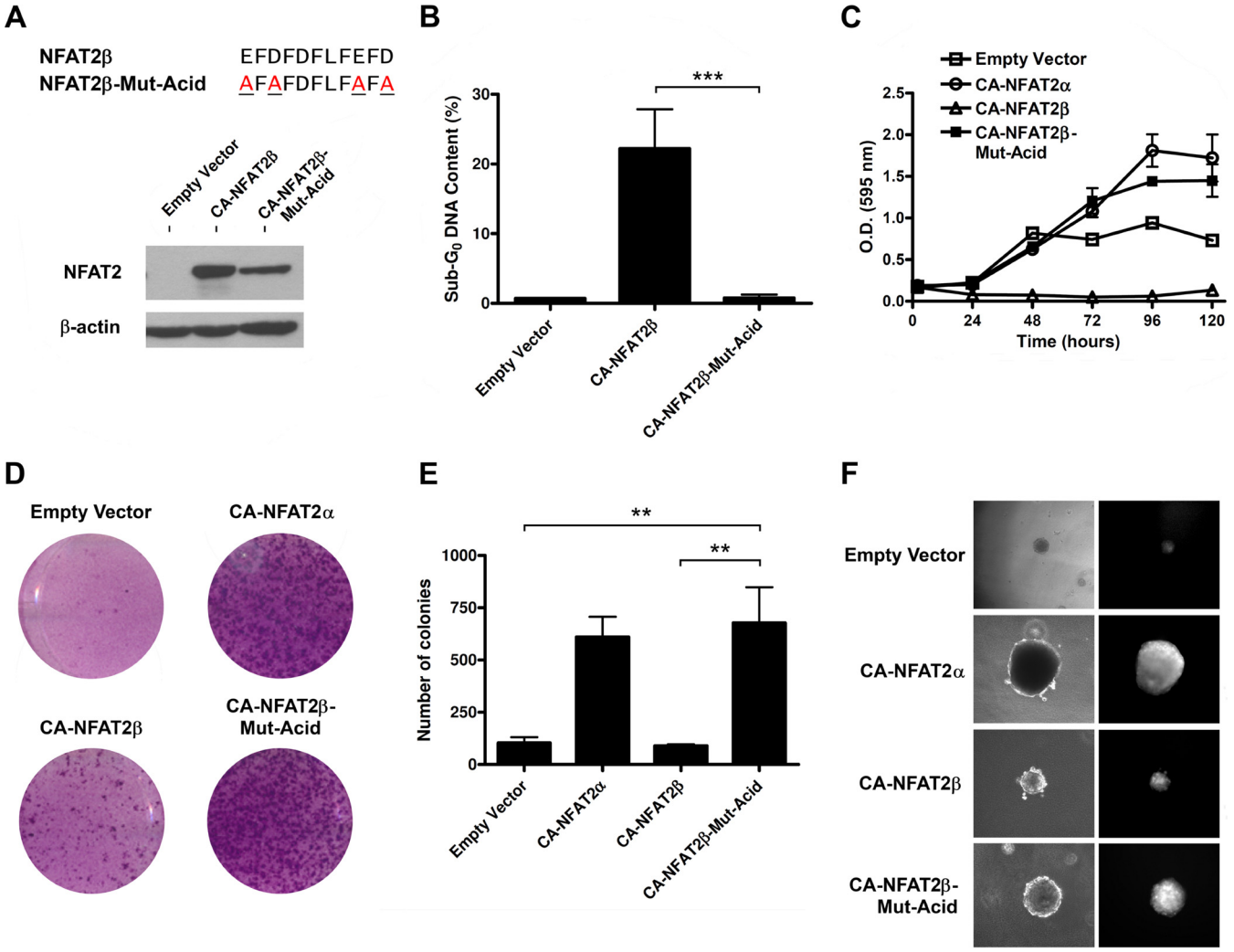

FIG 5 Substitution of the conserved acidic amino acids in the NFAT2β acidic activation domain completely abolishes cell death and enhances the cell transformation phenotype. NIH 3T3 cells were retrovirally transduced with the indicated vectors. (A, top) CA-NFAT2β-Mut-Acid was constructed by substitution of 4 acidic amino acids residues, E9A, D11A, E17A, and D19A. (Bottom) Expression levels of the CA-NFAT2 constructs were analyzed by Western blotting. (B) Cell death was assessed by sub-G_0 DNA content analysis as described in the legend to Fig. 3D. *** indicates a *P* value of ≤0.001. (C and D) Proliferation kinetics assays (C) and focus-forming assays (D) were performed as described in the legend to Fig. 1C and 2A, respectively. (E and F) Growth in semisolid medium was assessed as described in the legend to Fig. 2C and D. ** indicates a *P* value of ≤0.01. All results are representative of data from at least three independent experiments.

or NFAT2α protein, respectively (7, 24). These variants may also display different C termini by alternative splicing (3, 7, 37, 38). The regulatory mechanisms of NFAT2 isoform expression are well described for lymphocytes. NFAT2 transcription is controlled by two promoters, P1 and P2 (24). In T lymphocytes, only P1 is an NFAT-dependent inducible promoter, while P2 regulates the constitutive basal expression of NFAT2. NFAT binding to the P1 promoter induces transcription from exon 1 and splicing to exon 3, leading to the massive synthesis of the NFAT2α isoform (24, 38, 39). In contrast, the P2 promoter controls basal transcription of NFAT2β from exon 2 (24, 25). Interestingly, NFAT2 is the only inducible NFAT family gene regulated at the transcriptional level through an autoregulatory loop. Upon T cell receptor (TCR) engagement and NFAT protein activation, the autoregulatory loop leads to the massive expression of NFAT2α, exceeding the expression levels of the NFAT2β isoform several times (24). The regulation of the NFAT2 isoforms is similar in B cells upon anti-IgM stimulation (26, 27). The presence of the NFAT2 autoregulatory loop and NFAT2α upregulation protect both T and B cells from activation-induced cell death (AICD) (24, 26). NFAT2α might work as an important regulator of genes involved in cell survival and proliferation without efficiently affecting cell death genes. Alternatively, NFAT2α could compete with NFAT2β for the promoter regions of cell death genes, preventing premature death in activated T or B cells. Once the NFAT2α levels decrease after stimulus reduction, NFAT2β could contribute to AICD through the upregulation of cell death genes such as the FasL and TNF-α genes.

The transactivation activity of the TAD-N could explain the different phenotypes induced by the NFAT2 isoforms. N-terminal transactivation activity was observed for several NFAT family

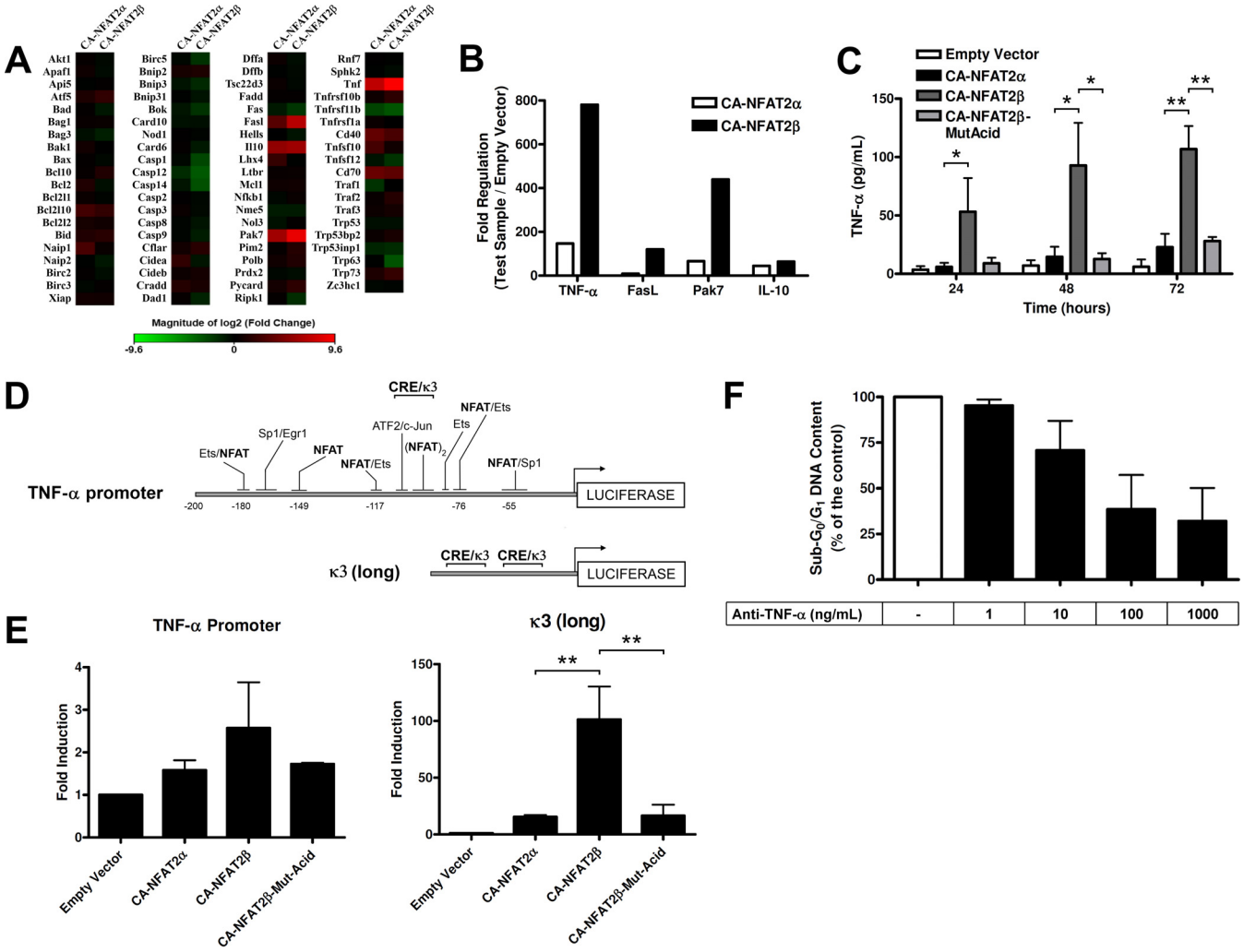

FIG 6 CA-NFAT2β induces death in NIH 3T3 cells by upregulation of TNF-α. NIH 3T3 cells were transduced with the empty vector or vectors containing CA-NFAT2α, CA-NFAT2β, or CA-NFAT2β-Mut-Acid. (A and B) A real-time reverse transcriptase (SYBR green) SuperArray assay was performed to screen 81 apoptosis-related genes. The fold change values are relative to the values for cells transduced with the empty vector. (C) TNF-α ELISA. Transduced cells were plated, and the cell-free supernatant was assessed for TNF-α protein levels by an ELISA at the indicated times. Data are shown as means ± standard deviations of results from three independent experiments. (D) Schematic representation of luciferase reporter vectors. Transcription factor-binding sites are indicated. (E) NIH 3T3 cells were transfected with the luciferase reporter plasmids and pRL-TK (renilla plasmid) and transduced with retroviral vectors. Transduced cells were plated at confluence and lysed after 16 h. Luciferase activity was normalized to the activity of the renilla vector. The fold induction values are relative to the values for cells transduced with the empty vector. Data are shown as the means ± standard deviations of data from three independent experiments. ** indicates a *P* value of ≤0.01. (F) Neutralization assay. NIH 3T3 cells were infected with the pLIRES-CA-NFAT2β vector and plated with a TNF-α neutralizing antibody. After 72 h, cell death was analyzed by PI staining. Data were normalized and expressed as a percentage relative to the sub-G_0 DNA content of nontreated cells. Standard deviation values indicate the variance of data from five independent experiments.

members that contain the N-terminal acidic domain. One-hybrid assays have shown that the region spanning aa 1 to 30 of NFAT2β containing the acidic domain is necessary and sufficient for eliciting a high activation signal (28). Similarly, the regions spanning aa 1 to 144 and aa 1 to 217 of NFAT1 and NFAT3, respectively, showed high transactivation activity (40, 41). Accordingly, the NFAT2α fragments spanning aa 1 to 44 and aa 1 to 106 that do not contain the N-terminal acidic domain were unable to induce transcription (28, 37). Moreover, it was shown previously that NFAT2β is able to induce greater IL-4 transactivation than NFAT2α (28), suggesting that the different N termini of the NFAT2 proteins might be important for IL-4 regulation. Our data demonstrate that NFAT2β can induce greater expression of several genes than NFAT2α (Fig. 6). Taken together, these data suggest a functional relevance for the different isoforms and alternative NFAT exon usage, where isoforms that maintain the conserved AAD could activate transcription through their TAD-Ns.

Furthermore, our data suggest a remarkably differential role of the NFAT2 isoforms in the regulation of cell death through the upregulation of TNF-α (Fig. 1, 6, and 7E). Previous studies have shown the differential regulation of TNF-α by NFAT proteins. Whereas the NFAT1 protein was able to bind to and transactivate the TNF-α promoter, leading to increased expression of this pro-apoptotic protein, the NFAT2 protein was unable to transactivate the TNF-α promoter (42, 43). However, in both studies, only the NFAT2α isoform was analyzed. One-hybrid assays have shown

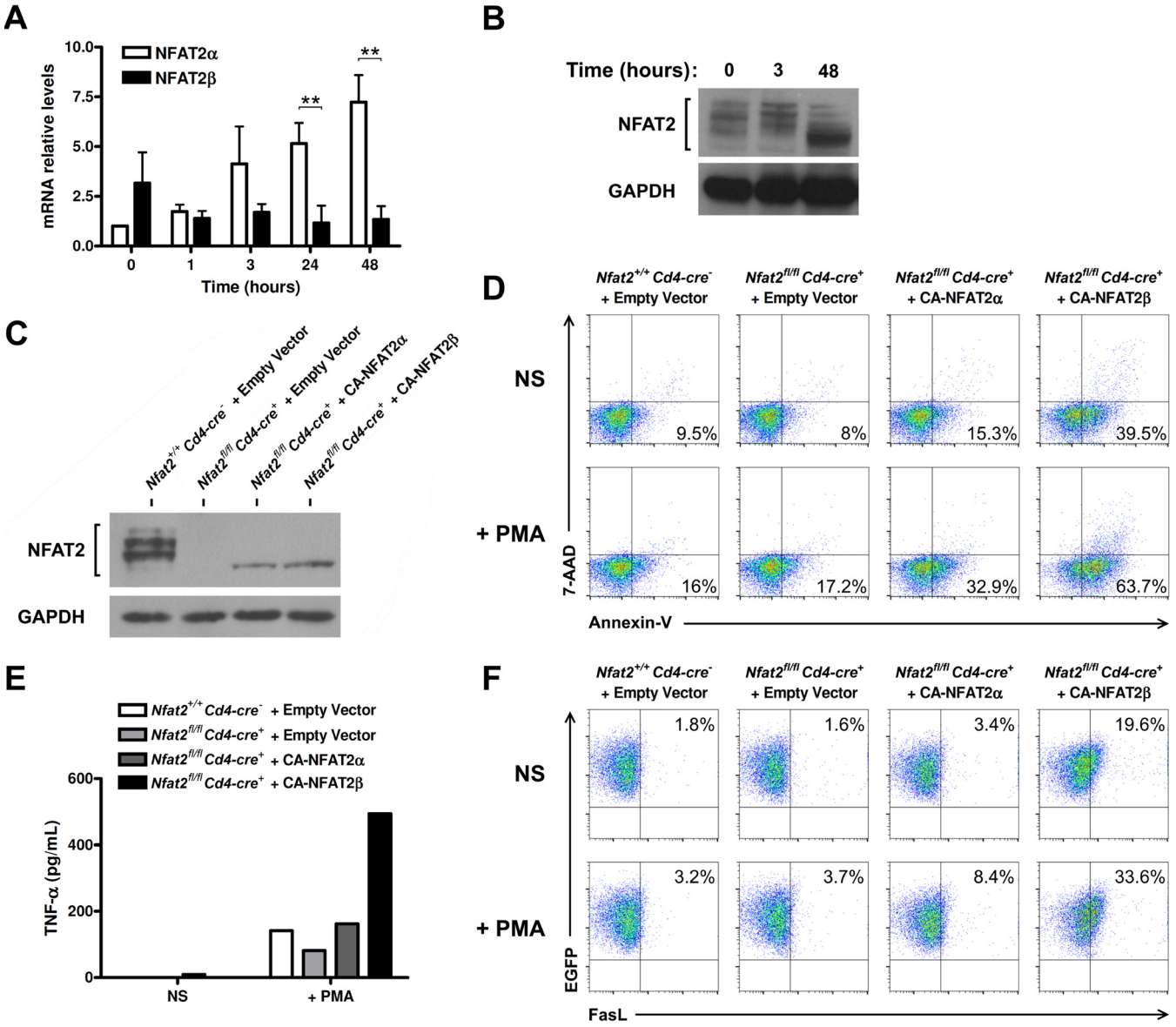

FIG 7 CA-NFAT2β induces cell death and increases FasL and TNF-α levels in CD4$^+$ T lymphocytes. (A) Analysis of mRNA levels of NFAT2 isoforms in primary CD4$^+$ T cells. Cells were stimulated with anti-CD3 and anti-CD28 (both at 1 μg/ml) for the indicated times, and mRNA levels of NFAT2 isoforms were analyzed by a real-time RT-PCR assay using SYBR green master mix. The data were normalized to hypoxanthine-guanine phosphoribosyltransferase levels. The fold change values are relative to the NFAT2α levels at the starting point (0 h). Data are shown as means ± standard deviations of results from three independent experiments. ** indicates a *P* value of ≤0.01. (B) Western blotting for NFAT2 and GAPDH (glyceraldehyde-3-phosphate dehydrogenase) levels in CD4$^+$ T cells stimulated with anti-CD3 and anti-CD28 for the indicated times. (C) Western blotting of transduced CD4$^+$ T cells. CD4$^+$ T cells were purified from *Nfat2*$^{+/+}$ *Cd4-cre*$^-$ (wild-type cells) or *Nfat2*$^{fl/fl}$ *Cd4-cre*$^+$ (*Nfat2*$^{-/-}$ cells) mice and transduced with the empty vector or vectors containing CA-NFAT2α or CA-NFAT2β. (D) Cell death analysis by annexin V and 7-AAD staining. Cells were plated in the absence (nonstimulated [NS]) or presence of 10 nM PMA. After 6 h, phosphatidylserine exposure was accompanied by annexin V staining. The data are representative of results from two independent experiments. (E) TNF-α ELISA. Transduced CD4$^+$ T cells were plated, and the cell-free supernatant was assessed for TNF-α protein levels by an ELISA after 6 h. Data are shown as means of results from two independent experiments. (F) FasL staining. Cells were plated in the absence or presence of 10 nM PMA for 6 h and stained with anti-FasL-PE antibody. The data are representative of results from two independent experiments.

that the TAD-C of NFAT1 contains a strong transcription activation domain (44), and its fusion to NFAT2α allowed this isoform to transactivate the TNF-α gene in Jurkat cells (43) and to induce death in NIH 3T3 cells (45). Here, we suggest that NFAT2 requires a transactivation domain to regulate TNF-α expression. Mechanistically, the use of exon 2 in NFAT2β may enable this isoform to induce TNF-α expression because it contains a potent transactivation element. Similarly, our data show that CA-NFAT2β can increase FasL levels in both NIH 3T3 fibroblasts (data not shown) and CD4$^+$ T lymphocytes (Fig. 7F). The upregulation of FasL was not sufficient for cell death induction in NIH 3T3 cells (data not shown) but is fundamental for AICD of T cells (46). Together, our results indicate that NFAT2β can regulate cell death in different cell types through two apoptosis inducers, suggesting a relevant

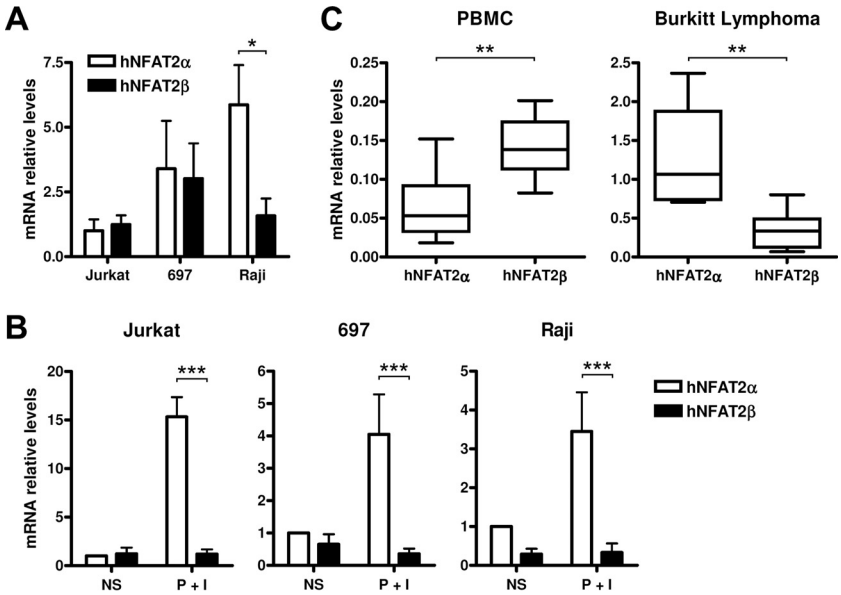

FIG 8 NFAT2 isoforms are differentially expressed in human cancer cell lines and Burkitt lymphoma samples. Total RNAs from the cancer cell lines Jurkat (T cell leukemia), 697 (pre-B cell leukemia), and Raji (Burkitt lymphoma); peripheral blood mononuclear cells (PBMC); or Burkitt lymphoma samples were isolated, and mRNA levels of human NFAT2 (hNFAT2) isoforms were analyzed by a real-time RT-PCR assay using SYBR green master mix. The data were normalized to phosphoglycerate kinase 1 and TATA-binding protein levels. (A) Comparison of levels of the NFAT2 isoforms in cultured cell lines. The fold change values are relative to the levels of human NFAT2α in Jurkat cells. Standard deviation values indicate the variance of data from five independent experiments. * indicates a *P* value of ≤0.05. (B) Analysis of NFAT2 levels after stimulation. Cell lines were treated with PMA (10 nM) plus ionomycin (1 μM) (P + I) for 4 h. The fold change values are relative to levels of human NFAT2α in nonstimulated (NS) cells. Data are shown as means ± standard deviations of results from at least four independent experiments. *** indicates a *P* value of ≤0.001. (C) Evaluation of NFAT2 mRNA levels in PBMCs ($n = 10$) or Burkitt lymphoma samples ($n = 7$). The mRNA levels are relative to the mRNA levels of housekeeping genes (phosphoglycerate kinase 1 and TATA-binding protein genes). ** indicates a *P* value of ≤0.01 (as determined by a Mann-Whitney U test).

proapoptotic role. Interestingly, an autoregulatory loop also was suggested for NFAT3 in nonimmune cells (47), and it was shown that NFAT3 has an antioncogenic role in NIH 3T3 cells (48). Therefore, the possible upregulation of NFAT3 by CA-NFAT2β could contribute to distinct oncogenic roles of NFAT2 isoforms in NIH 3T3 cells.

Since NFAT2β can regulate proapoptotic genes, this isoform may acts as an antioncogenic factor, displaying a possible tumor suppressor role. However, several studies indicate an important role of NFAT2 in cell transformation. It has been demonstrated that the sustained activity of NFAT2 is able to induce transformation hallmarks (Fig. 2) (9, 49) and is linked to some malignant transformations, such as Burkitt lymphoma, DLBCL, T-cell acute lymphoblastic leukemia ((T-ALL), CLL, melanoma, and pancreatic and colorectal carcinomas (11, 20–23, 50). NFAT2 also regulates genes important for tumorigenesis and tumor development, including those for c-myc, BLyS, and Cox-2 (11, 51–53). These apparently controversial data might be explained by the lack of data showing the differential expression of NFAT2α and NFAT2β in these tumors.

Our data showed that NFAT2α expression was increased in comparison to NFAT2β expression in Burkitt lymphoma cells (Fig. 8), suggesting that this specific isoform could be involved in tumor formation. Although our study is limited by its small sample size, it gives support to future studies with large numbers of patients where the relationship between the differential expression of the NFAT2 isoforms and the different aspects of cancer development, including the stage, invasiveness, and outcome, could be addressed. Since NFAT2α and NFAT2β may play differential roles in cellular functions, deregulation of isoform expression could contribute to tumorigenesis. During cell lineage differentiation, some transcription factors can employ positive autoregulatory mechanisms of one specific isoform to guarantee high levels of the protein to enable the maintenance of a differentiated state (54). This mechanism might account for the establishment of a lymphocyte activation-committed state through the overexpression of the NFAT2α protein and might also be exploited by tumor cells to induce a transformed commitment state. Taken together, our results suggest a novel regulation of the NFAT proteins through the alternative usage of initiation exons and define the NFAT2 transcription factors as dual regulators of cell transformation. These findings suggest that NFAT2α expression may be a potential therapeutic target. Since the NFAT2 signaling pathway seems to be important in several tumors, specific inhibition of the tumorigenic part of NFAT2 signaling while maintaining its tumor-suppressive abilities may be a good strategy for the treatment of cancer.

ACKNOWLEDGMENTS

We are especially grateful to A. Rao for kindly providing the NFAT reagents and *Nfat2*$^{fl/fl}$ *Cd4-cre*$^{+}$ mice.

This work was supported by grants to J.P.B.V. from the CNPq (307296/2011-3 and 476314/2012-7), FAPERJ (112.056/2012, 102.308/2013, 110.794/2013, and 101.147/2013), and INCT-Cancer (573806/2008-0 and 170.026/2008). P.I.L. and D.V.F. were supported by a FAPERJ fellowship, M.C.R. was supported by a CAPES fellowship, and E.P. was supported by a CNPq fellowship.

FUNDING INFORMATION

Conselho Nacional de Desenvolvimento Científico e Tecnológico (CNPq) provided funding to Joao P. B. Viola under grant numbers 307296/2011-3 and 476314/2012-7. Fundação Carlos Chagas Filho de Amparo à Pesquisa do Estado do Rio de Janeiro (FAPERJ) provided funding to Joao P. B. Viola under grant numbers 112.056/2012, 102.308/2013, 110.794/2013, and 101.147/2013. Instituto Nacional de Ciência e Tecnologia para o Controle do Câncer (INCT-Cancer) provided funding to Joao P. B. Viola under grant numbers 573806/2008-0 and 170.026/2008.

REFERENCES

1. **Shaw JP, Utz PJ, Durand DB, Toole JJ, Emmel EA, Crabtree GR.** 1988. Identification of a putative regulator of early T cell activation genes. Science **241:**202–205. http://dx.doi.org/10.1126/science.3260404.
2. **McCaffrey PG, Perrino BA, Soderling TR, Rao A.** 1993. NF-ATp, a T lymphocyte DNA-binding protein that is a target for calcineurin and immunosuppressive drugs. J Biol Chem **268:**3747–3752.
3. **Northrop JP, Ho SN, Chen L, Thomas DJ, Timmerman LA, Nolan GP, Admon A, Crabtree GR.** 1994. NF-AT components define a family of transcription factors targeted in T-cell activation. Nature **369:**497–502. http://dx.doi.org/10.1038/369497a0.
4. **Hoey T, Sun YL, Williamson K, Xu X.** 1995. Isolation of two new members of the NF-AT gene family and functional characterization of the NF-AT proteins. Immunity **2:**461–472. http://dx.doi.org/10.1016/1074-7613(95)90027-6.
5. **Masuda ES, Naito Y, Tokumitsu H, Campbell D, Saito F, Hannum C, Arai K, Arai N.** 1995. NFATx, a novel member of the nuclear factor of activated T cells family that is expressed predominantly in the thymus. Mol Cell Biol **15:**2697–2706. http://dx.doi.org/10.1128/MCB.15.5.2697.
6. **Rao A, Luo C, Hogan PG.** 1997. Transcription factors of the NFAT family: regulation and function. Annu Rev Immunol **15:**707–747. http://dx.doi.org/10.1146/annurev.immunol.15.1.707.
7. **Vihma H, Pruunsild P, Timmusk T.** 2008. Alternative splicing and expression of human and mouse NFAT genes. Genomics **92:**279–291. http://dx.doi.org/10.1016/j.ygeno.2008.06.011.
8. **Macian F.** 2005. NFAT proteins: key regulators of T-cell development and function. Nat Rev Immunol **5:**472–484. http://dx.doi.org/10.1038/nri1632.
9. **Robbs BK, Cruz AL, Werneck MB, Mognol GP, Viola JP.** 2008. Dual roles for NFAT transcription factor genes as oncogenes and tumor suppressors. Mol Cell Biol **28:**7168–7181. http://dx.doi.org/10.1128/MCB.00256-08.
10. **Viola JP, Carvalho LD, Fonseca BP, Teixeira LK.** 2005. NFAT transcription factors: from cell cycle to tumor development. Braz J Med Biol Res **38:**335–344. http://dx.doi.org/10.1590/S0100-879X2005000300003.
11. **Buchholz M, Schatz A, Wagner M, Michl P, Linhart T, Adler G, Gress TM, Ellenrieder V.** 2006. Overexpression of c-myc in pancreatic cancer caused by ectopic activation of NFATc1 and the Ca2+/calcineurin signaling pathway. EMBO J **25:**3714–3724. http://dx.doi.org/10.1038/sj.emboj.7601246.
12. **Mognol GP, de Araujo-Souza PS, Robbs BK, Teixeira LK, Viola JP.** 2012. Transcriptional regulation of the c-Myc promoter by NFAT1 involves negative and positive NFAT-responsive elements. Cell Cycle **11:**1014–1028. http://dx.doi.org/10.4161/cc.11.5.19518.
13. **Carvalho LD, Teixeira LK, Carrossini N, Caldeira AT, Ansel KM, Rao A, Viola JP.** 2007. The NFAT1 transcription factor is a repressor of cyclin A2 gene expression. Cell Cycle **6:**1789–1795. http://dx.doi.org/10.4161/cc.6.14.4473.
14. **Pedrosa AM, Weinlich R, Mognol GP, Robbs BK, Viola JP, Campa A, Amarante-Mendes GP.** 2010. Melatonin protects $CD4^+$ T cells from activation-induced cell death by blocking NFAT-mediated CD95 ligand upregulation. J Immunol **184:**3487–3494. http://dx.doi.org/10.4049/jimmunol.0902961.
15. **Youn HD, Chatila TA, Liu JO.** 2000. Integration of calcineurin and MEF2 signals by the coactivator p300 during T-cell apoptosis. EMBO J **19:**4323–4331. http://dx.doi.org/10.1093/emboj/19.16.4323.
16. **Zaichuk TA, Shroff EH, Emmanuel R, Filleur S, Nelius T, Volpert OV.** 2004. Nuclear factor of activated T cells balances angiogenesis activation and inhibition. J Exp Med **199:**1513–1522. http://dx.doi.org/10.1084/jem.20040474.
17. **Robbs BK, Lucena PI, Viola JP.** 2013. The transcription factor NFAT1 induces apoptosis through cooperation with Ras/Raf/MEK/ERK pathway and upregulation of TNF-alpha expression. Biochim Biophys Acta **1833:**2016–2028. http://dx.doi.org/10.1016/j.bbamcr.2013.04.003.
18. **Medyouf H, Ghysdael J.** 2008. The calcineurin/NFAT signaling pathway: a novel therapeutic target in leukemia and solid tumors. Cell Cycle **7:**297–303. http://dx.doi.org/10.4161/cc.7.3.5357.
19. **Qin JJ, Nag S, Wang W, Zhou J, Zhang WD, Wang H, Zhang R.** 2014. NFAT as cancer target: mission possible? Biochim Biophys Acta **1846:**297–311. http://dx.doi.org/10.1016/j.bbcan.2014.07.009.
20. **Levin-Gromiko U, Koshelev V, Kushnir P, Fedida-Metula S, Voronov E, Fishman D.** 2014. Amplified lipid rafts of malignant cells constitute a target for inhibition of aberrantly active NFAT and melanoma tumor growth by the aminobisphosphonate zoledronic acid. Carcinogenesis **35:**2555–2566. http://dx.doi.org/10.1093/carcin/bgu178.
21. **Tripathi MK, Deane NG, Zhu J, An H, Mima S, Wang X, Padmanabhan S, Shi Z, Prodduturi N, Ciombor KK, Chen X, Washington MK, Zhang B, Beauchamp RD.** 2014. Nuclear factor of activated T-cell activity is associated with metastatic capacity in colon cancer. Cancer Res **74:**6947–6957. http://dx.doi.org/10.1158/0008-5472.CAN-14-1592.
22. **Marafioti T, Pozzobon M, Hansmann ML, Ventura R, Pileri SA, Roberton H, Gesk S, Gaulard P, Barth TF, Du MQ, Leoncini L, Moller P, Natkunam Y, Siebert R, Mason DY.** 2005. The NFATc1 transcription factor is widely expressed in white cells and translocates from the cytoplasm to the nucleus in a subset of human lymphomas. Br J Haematol **128:**333–342. http://dx.doi.org/10.1111/j.1365-2141.2004.05313.x.
23. **Le Roy C, Deglesne PA, Chevallier N, Beitar T, Eclache V, Quettier M, Boubaya M, Letestu R, Levy V, Ajchenbaum-Cymbalista F, Varin-Blank N.** 2012. The degree of BCR and NFAT activation predicts clinical outcomes in chronic lymphocytic leukemia. Blood **120:**356–365. http://dx.doi.org/10.1182/blood-2011-12-397158.
24. **Chuvpilo S, Jankevics E, Tyrsin D, Akimzhanov A, Moroz D, Jha MK, Schulze-Luehrmann J, Santner-Nanan B, Feoktistova E, Konig T, Avots A, Schmitt E, Berberich-Siebelt F, Schimpl A, Serfling E.** 2002. Autoregulation of NFATc1/A expression facilitates effector T cells to escape from rapid apoptosis. Immunity **16:**881–895. http://dx.doi.org/10.1016/S1074-7613(02)00329-1.
25. **Sherman MA, Powell DR, Weiss DL, Brown MA.** 1999. NF-ATc isoforms are differentially expressed and regulated in murine T and mast cells. J Immunol **162:**2820–2828.
26. **Bhattacharyya S, Deb J, Patra AK, Thuy Pham DA, Chen W, Vaeth M, Berberich-Siebelt F, Klein-Hessling S, Lamperti ED, Reifenberg K, Jellusova J, Schweizer A, Nitschke L, Leich E, Rosenwald A, Brunner C, Engelmann S, Bommhardt U, Avots A, Muller MR, Kondo E, Serfling E.** 2011. NFATc1 affects mouse splenic B cell function by controlling the calcineurin-NFAT signaling network. J Exp Med **208:**823–839. http://dx.doi.org/10.1084/jem.20100945.
27. **Hock M, Vaeth M, Rudolf R, Patra AK, Pham DA, Muhammad K, Pusch T, Bopp T, Schmitt E, Rost R, Berberich-Siebelt F, Tyrsin D, Chuvpilo S, Avots A, Serfling E, Klein-Hessling S.** 2013. NFATc1 induction in peripheral T and B lymphocytes. J Immunol **190:**2345–2353. http://dx.doi.org/10.4049/jimmunol.1201591.
28. **Hock MB, Brown MA.** 2003. Nuclear factor of activated T cells 2 transactivation in mast cells: a novel isoform-specific transactivation domain confers unique FcepsilonRI responsiveness. J Biol Chem **278:**26695–26703. http://dx.doi.org/10.1074/jbc.M301007200.
29. **Martinez GJ, Pereira RM, Aijo T, Kim EY, Marangoni F, Pipkin ME, Togher S, Heissmeyer V, Zhang YC, Crotty S, Lamperti ED, Ansel KM, Mempel TR, Lahdesmaki H, Hogan PG, Rao A.** 2015. The transcription factor NFAT promotes exhaustion of activated CD8(+) T cells. Immunity **42:**265–278. http://dx.doi.org/10.1016/j.immuni.2015.01.006.
30. **Teixeira LK, Fonseca BP, Vieira-de-Abreu A, Barboza BA, Robbs BK, Bozza PT, Viola JP.** 2005. IFN-gamma production by $CD8^+$ T cells depends on NFAT1 transcription factor and regulates Th differentiation. J Immunol **175:**5931–5939. http://dx.doi.org/10.4049/jimmunol.175.9.5931.
31. **Monticelli S, Rao A.** 2002. NFAT1 and NFAT2 are positive regulators of IL-4 gene transcription. Eur J Immunol **32:**2971–2978. http://dx.doi.org/10.1002/1521-4141(2002010)32:10<2971::AID-IMMU2971>3.0.CO;2-G.
32. **Tsai EY, Jain J, Pesavento PA, Rao A, Goldfeld AE.** 1996. Tumor necrosis factor alpha gene regulation in activated T cells involves ATF-2/Jun and NFATp. Mol Cell Biol **16:**459–467. http://dx.doi.org/10.1128/MCB.16.2.459.
33. **Triezenberg SJ.** 1995. Structure and function of transcriptional activation

domains. Curr Opin Genet Dev **5:**190–196. http://dx.doi.org/10.1016/0959-437X(95)80007-7.
34. **Giniger E, Ptashne M.** 1987. Transcription in yeast activated by a putative amphipathic alpha helix linked to a DNA binding unit. Nature **330:**670–672. http://dx.doi.org/10.1038/330670a0.
35. **Falvo JV, Tsytsykova AV, Goldfeld AE.** 2010. Transcriptional control of the TNF gene. Curr Dir Autoimmun **11:**27–60. http://dx.doi.org/10.1159/000289196.
36. **Vaeth M, Schliesser U, Muller G, Reissig S, Satoh K, Tuettenberg A, Jonuleit H, Waisman A, Muller MR, Serfling E, Sawitzki BS, Berberich-Siebelt F.** 2012. Dependence on nuclear factor of activated T-cells (NFAT) levels discriminates conventional T cells from Foxp3+ regulatory T cells. Proc Natl Acad Sci U S A **109:**16258–16263. http://dx.doi.org/10.1073/pnas.1203870109.
37. **Chuvpilo S, Avots A, Berberich-Siebelt F, Glockner J, Fischer C, Kerstan A, Escher C, Inashkina I, Hlubek F, Jankevics E, Brabletz T, Serfling E.** 1999. Multiple NF-ATc isoforms with individual transcriptional properties are synthesized in T lymphocytes. J Immunol **162:**7294–7301.
38. **Chuvpilo S, Zimmer M, Kerstan A, Glockner J, Avots A, Escher C, Fischer C, Inashkina I, Jankevics E, Berberich-Siebelt F, Schmitt E, Serfling E.** 1999. Alternative polyadenylation events contribute to the induction of NF-ATc in effector T cells. Immunity **10:**261–269. http://dx.doi.org/10.1016/S1074-7613(00)80026-6.
39. **Zhou B, Cron RQ, Wu B, Genin A, Wang Z, Liu S, Robson P, Baldwin HS.** 2002. Regulation of the murine Nfatc1 gene by NFATc2. J Biol Chem **277:**10704–10711. http://dx.doi.org/10.1074/jbc.M107068200.
40. **Luo C, Burgeon E, Rao A.** 1996. Mechanisms of transactivation by nuclear factor of activated T cells-1. J Exp Med **184:**141–147. http://dx.doi.org/10.1084/jem.184.1.141.
41. **Yang T, Davis RJ, Chow CW.** 2001. Requirement of two NFATc4 transactivation domains for CBP potentiation. J Biol Chem **276:**39569–39576. http://dx.doi.org/10.1074/jbc.M102961200.
42. **Oum JH, Han J, Myung H, Hleb M, Sharma S, Park J.** 2002. Molecular mechanism of NFAT family proteins for differential regulation of the IL-2 and TNF-alpha promoters. Mol Cells **13:**77–84.
43. **Kaminuma O, Kitamura F, Kitamura N, Hiroi T, Miyoshi H, Miyawaki A, Miyatake S.** 2008. Differential contribution of NFATc2 and NFATc1 to TNF-alpha gene expression in T cells. J Immunol **180:**319–326. http://dx.doi.org/10.4049/jimmunol.180.1.319.
44. **Luo C, Burgeon E, Carew JA, McCaffrey PG, Badalian TM, Lane WS, Hogan PG, Rao A.** 1996. Recombinant NFAT1 (NFATp) is regulated by calcineurin in T cells and mediates transcription of several cytokine genes. Mol Cell Biol **16:**3955–3966. http://dx.doi.org/10.1128/MCB.16.7.3955.
45. **Faget DV, Lucena PI, Robbs BK, Viola JP.** 2012. NFAT1 C-terminal domains are necessary but not sufficient for inducing cell death. PLoS One **7:**e47868. http://dx.doi.org/10.1371/journal.pone.0047868.
46. **Green DR, Droin N, Pinkoski M.** 2003. Activation-induced cell death in T cells. Immunol Rev **193:**70–81. http://dx.doi.org/10.1034/j.1600-065X.2003.00051.x.
47. **Arron JR, Winslow MM, Polleri A, Chang CP, Wu H, Gao X, Neilson JR, Chen L, Heit JJ, Kim SK, Yamasaki N, Miyakawa T, Francke U, Graef IA, Crabtree GR.** 2006. NFAT dysregulation by increased dosage of DSCR1 and DYRK1A on chromosome 21. Nature **441:**595–600. http://dx.doi.org/10.1038/nature04678.
48. **Yao K, Cho YY, Bergen HR, III, Madden BJ, Choi BY, Ma WY, Bode AM, Dong Z.** 2007. Nuclear factor of activated T3 is a negative regulator of Ras-JNK1/2-AP-1 induced cell transformation. Cancer Res **67:**8725–8735. http://dx.doi.org/10.1158/0008-5472.CAN-06-4788.
49. **Neal JW, Clipstone NA.** 2003. A constitutively active NFATc1 mutant induces a transformed phenotype in 3T3-L1 fibroblasts. J Biol Chem **278:**17246–17254. http://dx.doi.org/10.1074/jbc.M300528200.
50. **Medyouf H, Alcalde H, Berthier C, Guillemin MC, dos Santos NR, Janin A, Decaudin D, de The H, Ghysdael J.** 2007. Targeting calcineurin activation as a therapeutic strategy for T-cell acute lymphoblastic leukemia. Nat Med **13:**736–741. http://dx.doi.org/10.1038/nm1588.
51. **Pham LV, Tamayo AT, Li C, Bueso-Ramos C, Ford RJ.** 2010. An epigenetic chromatin remodeling role for NFATc1 in transcriptional regulation of growth and survival genes in diffuse large B-cell lymphomas. Blood **116:**3899–3906. http://dx.doi.org/10.1182/blood-2009-12-257378.
52. **Fu L, Lin-Lee YC, Pham LV, Tamayo A, Yoshimura L, Ford RJ.** 2006. Constitutive NF-kappaB and NFAT activation leads to stimulation of the BLyS survival pathway in aggressive B-cell lymphomas. Blood **107:**4540–4548. http://dx.doi.org/10.1182/blood-2005-10-4042.
53. **Duque J, Fresno M, Iniguez MA.** 2005. Expression and function of the nuclear factor of activated T cells in colon carcinoma cells: involvement in the regulation of cyclooxygenase-2. J Biol Chem **280:**8686–8693. http://dx.doi.org/10.1074/jbc.M413076200.
54. **Hogan PG, Chen L, Nardone J, Rao A.** 2003. Transcriptional regulation by calcium, calcineurin, and NFAT. Genes Dev **17:**2205–2232. http://dx.doi.org/10.1101/gad.1102703.